International Journal of Fracture **54:** 117–130, 1992.

A fracture-mechanical theory of subcritical crack growth in ceramics

T. FETT
Kernforschungszentrum Karlsruhe, Institut für Material- und Festkörperforschung IV, D–7500 Karlsruhe, Germany

Received 15 November 1989; accepted in revised form 20 July 1990

Abstract. An interpretation is proposed of the power law describing the relation between subcritical crack growth rate and stress intensity factor. It is based on the idea that thermal transients both break and re-establish bonds. The effects, which occur during these processes are mathematically described using a Morse potential. Already the rough model employed provides enough information on bond breaking to understand the principle of subcritical crack growth.

1. Introduction

Subcritical crack growth is responsible for delayed failure of statically loaded components. In experimental investigations carried out with various materials it has been found that over a wide range of stress intensity factors K_I, the subcritical crack growth rate v is given by a power law:

$$v = AK_I^n \tag{1}$$

K_I is defined by

$$K_I = \sigma\sqrt{a}\,Y, \tag{2}$$

where σ denotes the stress and a the depth of a crack in a structure, and Y is the geometric correction factor dependent on the shape of the crack and the component.

Measurements by Evans [1] demonstrate for glass that this power law relation is satisfied over a comparatively wide range of values for K_I. In the literature a fairly large number of theoretical explanations are reported to describe measured data [2]–[6]. In these various attempts, the functional dependence $v = f(K_I)$ is always described – as a consequence of the Arrhenius equation – by exponential functions, the arguments of which are linear, quadratic, or mixed-quadratic functions of the stress intensity factor.

The objective of this investigation is to give a theoretical explanation for (1) as a development of ideas based on [7]. An attempt is made, using simple model-based considerations, to arrive at an interpretation of the power law of subcritical crack growth. The interpretation starts from the idea that thermal transients both break and re-establish bonds.

2. Fracture-mechanical model

2.1. Displacements and stresses during a bond break

Before describing the fracture mechanical model two simple limit cases are considered. An isolated bond is mechanically loaded by springs, which simulate the elastic surrounding in a solid. In the first case (Fig. 1), the force F_{appl} is applied in a load-controlled manner symbolized by a dead weight. The bond reaction force F_{bond} has to be in equilibrium with the external load and it holds that $F_{bond} = F_{appl}$. This condition is fulfilled for an elongation $\delta^{(1)}$. In the case of a thermal transient with sufficiently high energy, which exceeds the potential barrier ΔU, the displacement between the bond partners exceeds the value $\delta^{(2)}$, shown in Fig. 1. Since now the constant applied force is higher than the bond forces, the model bond is completely cracked.

The second case of Fig. 1 is a displacement-controlled external load characterised by stretched springs fixed at their ends. In the case of a thermal transient splitting the bond, the external load becomes reduced with increasing distance of the two bond partners. If C is the spring stiffness, the external load is displacement dependent and it holds that $F_{appl} = F_{appl}(\delta^{(1)}) - C(\delta - \delta^{(1)})$. This linearly decreasing external load is illustrated in Fig. 1. It is obvious that in this case a second state of equilibrium is established at point $\delta^{(3)}$. Complete bond break is not possible.

In a real component containing a crack the load-displacement behaviour at the crack tip is much more complex than the two limit cases. In Fig. 2 the situation during a bond break at the tip of a crack with the crack depth a loaded by a constant stress σ_0 is illustrated. To allow

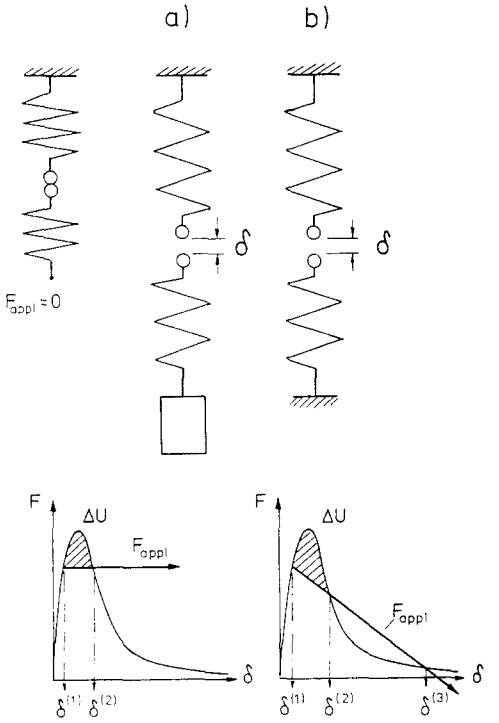

Fig. 1. Limit cases for bond breaking.

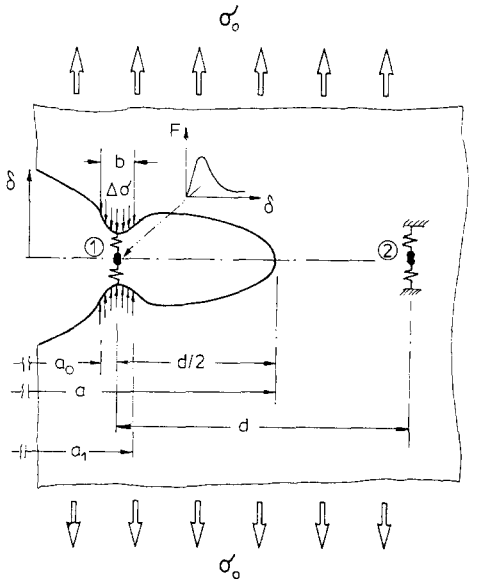

Fig. 2. Crack tip model.

a simple treatment only a linear model of the crack is chosen, i.e. the 'width' of the model specimen is equal to the distance d of bonds.

The load-displacement characteristic of a single bond is given by the F-δ-diagram in Fig. 2. The 'crack tip' of the model crack is assumed to be located in the center $d/2$ between the mostly stressed bond (1) and the next moderately stressed bond (2), as shown in Fig. 2. To allow application of continuum mechanics the single forces $F(\delta)$ are replaced by stresses $\Delta\sigma$ assumed to be constant over the range b. Therefore, the effective stresses are reduced by

$$\Delta\sigma = \frac{F(\delta)}{bd}, \tag{3}$$

where the factor d in the area bd is standing for the distance of the next collinear row of bonds. The stress distribution governing the crack-opening displacement field is then given as

$$\sigma = \begin{cases} \sigma_0 - \Delta\sigma & \text{for} \quad a_0 \leqslant x \leqslant a_1 \\ \sigma_0 & \text{else} \end{cases}, \tag{4}$$

where

$$a_0 = a - \frac{d}{2} - \frac{b}{2} \quad \text{and} \quad a_1 = a - \frac{d}{2} + \frac{b}{2}.$$

The weight function method provides a possibility to calculate the crack opening displacement field. The fracture mechanical weight function h [8] relates the stress intensity factor K_I to the stresses σ by

$$K_I = \int_0^a h(x, a)\sigma(x)\,\mathrm{d}x \tag{5a}$$

and can be derived from the crack opening displacement field of any reference loading case by [9]

$$h(x, a) = \frac{E}{K_I} \frac{\partial \delta}{\partial a} \tag{5b}$$

with Young's modulus E. Integration of (5b) gives a formula to calculate the crack-opening displacement field

$$\delta(x, a) = \frac{1}{E} \int_0^a \int_{\max(c,x)}^a \sigma(c) h(x, a') \mathrm{h}(\mathrm{c}, \mathrm{a}')\, \mathrm{d}a'\, \mathrm{d}c. \tag{6}$$

In this equation c denotes the location where the stress σ is applied and x is the location where the displacement δ is observed.

The crack-opening displacement field near the crack tip is related to the stress intensity factor by the well-known relation (see for example [10])

$$\delta(x \to a) = \sqrt{\frac{8}{\pi}} \frac{K_I}{E} \sqrt{a - x} \tag{7}$$

leading to the weight function

$$h(x, a) = \sqrt{\frac{2}{\pi(a - x)}}. \tag{8}$$

Introducing (2, 4, 8) into (6) yields

$$\delta = \delta_0 - \frac{2\Delta\sigma a}{\pi E} \left[g\left(\frac{x}{a}, \frac{a_0}{a}\right) - g\left(\frac{x}{a}, \frac{a_1}{a}\right) \right] \tag{9}$$

with

$$g\left(\frac{x}{a}, \frac{a_i}{a}\right) = 2\sqrt{1 - (x/a)^2} \arccos \frac{a_0}{a} - \frac{x}{a} \ln \frac{x - a_0 z}{x + a_0 z} + \frac{a_0}{a} \ln \frac{1 - z}{1 + z}, \tag{9a}$$

$$z = \sqrt{\frac{1 - (x/a)^2}{1 - (a_i/a)}} \tag{9b}$$

and

$$\delta_0 = \sqrt{8/\pi}\, \frac{\sigma_0}{E}\, Y \cdot a \sqrt{1 - \frac{x}{a}}. \tag{9c}$$

The crack-tip displacement field given by (9) is illustrated in Fig. 2 for $b/d = 0.2$. Especially for $x = a - d/2$ and $d, b \ll a$ it results

$$\delta\left(a - \frac{d}{2}\right) \to \delta_0 - \frac{2\Delta\sigma}{\pi E} d\left(2.296 - \ln\frac{b}{d}\right) \tag{10}$$

$$\delta_0 = \frac{2}{\sqrt{\pi}} \frac{\sigma_0}{E} Y \sqrt{a}\sqrt{d} = \frac{2}{\sqrt{\pi}} \frac{K_I}{E} \sqrt{d}. \tag{10a}$$

2.2 Effective forces during bond breaking

The *Morse potential* describes the energies of intermolecular bonds and has the form

$$U(\delta) = U_0[\exp(-2s\delta) - 2\exp(-s\delta)], \tag{11}$$

where $U(\delta)$ is the potential for a displacement δ, U_0 the dissociation energy and s is a measure of the range of bond forces. By differentiating (11), the force law becomes

$$F(\delta) = 2U_0 s[\exp(-s\delta) - \exp(-2s\delta)]. \tag{12}$$

Figure 3 shows how the force varies as a function of the displacement from the equilibrium position. The maximum force F_0 is reached when $s\delta = \ln 2$, so that (12) can be written as

$$F(\delta) = 4F_0[\exp(-s\delta) - \exp(-2s\delta)]. \tag{13}$$

If a body has the temperature T, the bonds can be broken by thermal transients of sufficiently high energy. A characterisation of the energy relationships involved in the thermal breakage of the near crack-tip bond is given in Fig. 3.

From (3), (10) and (13) it follows

$$\delta = \delta_0 - \frac{4F_0}{B}(e^{-s\delta} - e^{-2s\delta}), \tag{14}$$

where the constant factor B is given by

$$B = \frac{\pi E b}{2\left(2.296 - \ln\frac{b}{d}\right)}. \tag{15}$$

Equation (14) shows a different number of solutions dependent on the applied stress σ_0, which governs the value of δ_0. For small stresses (Fig. 3a) only one solution (called $\delta^{(1)}$) exists, which represents the state of equilibrium. Even when thermal transients with high energies occur, no additional state of equilibrium will be possible, and the bond will be re-established without a new thermal transient. In this case, the bond cannot be broken permanently.

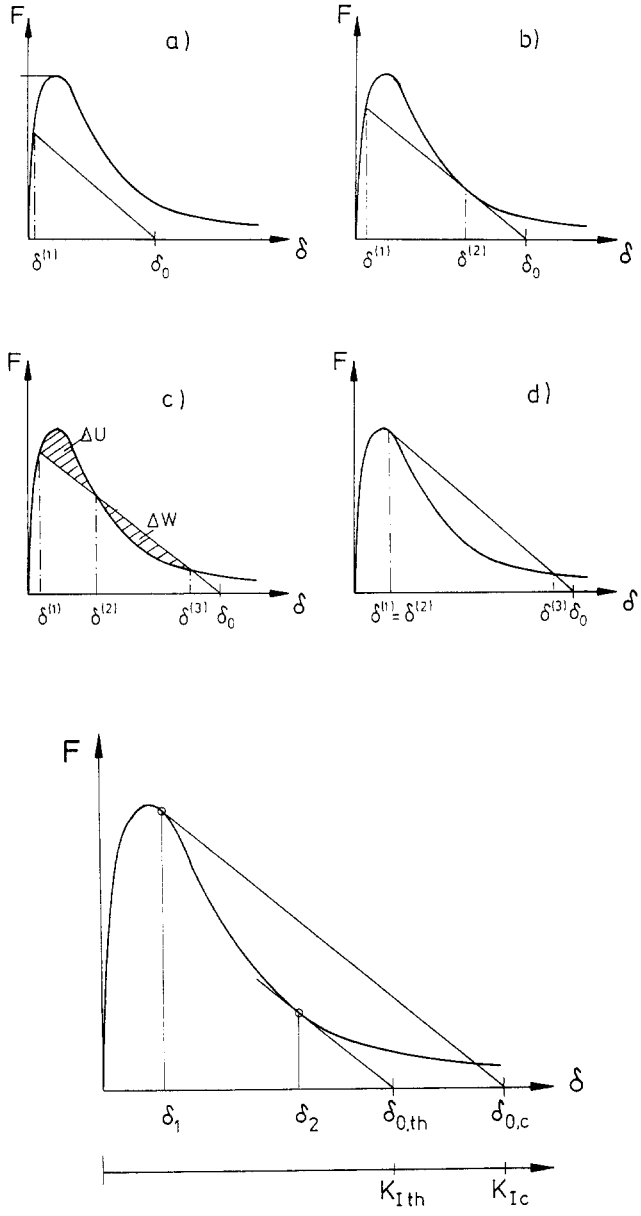

Fig. 3. Load displacement behaviour of a bond at the crack tip.

At an increased stress, (Fig. 3b), (14) has a second solution $\delta^{(2)}$, and at higher stresses (Fig. 3c) a third solution is found $\delta^{(3)}$. If in this case a thermal transient with an energy of at least ΔU occurs, the bond will find a new position of equilibrium at $\delta^{(3)}$ and the crack will increase by the increment $\Delta a = d$. This new situation is not necessarily a permanent one. If further thermal transients with energies of at least ΔW act at the considered location the bond can be re-established.

Figure 3d describes a critical load situation. The solutions $\delta^{(1)}$ and $\delta^{(2)}$ are identical and the straight line is the tangent to the bond force curve.

Figure 3b describes a limit situation leading to a threshold in bond breaking.

2.3. Determination of the critical and threshold values for crack opening and stress intensity factor

The two limit cases leading to a critical and a threshold value are described by those situations in which the straight lines in Fig. 3e are tangent to the bond force. In those cases it holds

$$\frac{dF}{d(s\delta)} = -4F_0[e^{-s\delta} - 2e^{-2s\delta}] = -\frac{B}{s}. \tag{16}$$

The two solutions are

$$(s\delta)_{1/2} = -\ln\left[\frac{1}{4}\left(1 \pm \sqrt{1 - \frac{2B}{sF_0}}\right)\right] \tag{17}$$

with the related forces

$$F_1 = \frac{F_0}{2}\left[1 + \sqrt{1 - \frac{2B}{sF_0}} + \frac{B}{sF_0}\right], \tag{18a}$$

$$F_2 = \frac{F_0}{2}\left[1 - \sqrt{1 - \frac{2B}{sF_0}} + \frac{B}{sF_0}\right]. \tag{18b}$$

If the crack opening δ_0 corresponding to the threshold situation is denoted by $\delta_{0,\mathrm{th}}$ and in the critical case by $\delta_{0,c}$ it holds that

$$\delta_{0,\mathrm{th}} = \frac{F_2}{B} + \delta_2, \tag{19a}$$

$$\delta_{0,c} = \frac{F_1}{B} + \delta_1. \tag{19b}$$

By taking into account (10a) one can express δ_0 by K_I

$$\frac{\delta_0}{\delta_{0,c}} = \frac{K_\mathrm{I}}{K_{\mathrm{I}c}}, \quad \frac{\delta_{0,\mathrm{th}}}{\delta_{0,c}} = \frac{K_{\mathrm{I}\mathrm{th}}}{K_{\mathrm{I}c}}. \tag{20}$$

2.4. Calculation of the potential barriers

The probability of occurrence of thermal transients with energies high enough for bond breaking is described by the Boltzmann distribution, namely

$$\bar{N}/N_0 = \exp(-\Delta U/kT). \tag{21}$$

In the expression $\bar{N}/N_0$ is the fraction of the transients with energies greater than ΔU, k is Boltzmann's constant and ΔU is the potential barrier which must be overcome.

For describing the frequency of bond-breaking events the knowledge of the potential barriers ΔU and ΔW is necessary. In case of $B \to 0$ the barrier ΔU can be evaluated analytically. This was shown in [7] and is outlined in the Appendix. The general case $B \neq 0$ has to be treated numerically.

The interdependency of the values F_{th}, F_c and the constant B is given by (18, 19). In Fig. 4 the resulting relative energies $\Delta U/U_0$ and $\Delta W/U_0$ are plotted versus the relative stress intensity factors K_I/K_{Ic} for $K_{Ith}/K_{Ic} = 0.25$.

Figure 5 shows the potential barrier ΔU as a function of $\ln(K_I/K_{Ic})$ at different values of K_{Ith}/K_{Ic}. From this representation a nearly linear behaviour can be concluded. Over a wide range of K_I/K_{Ic}, it is consequently possible to adopt the representation

$$\frac{\Delta U}{U_0} = A_0 + A_1 \ln \frac{K_I}{K_{Ic}}. \tag{22}$$

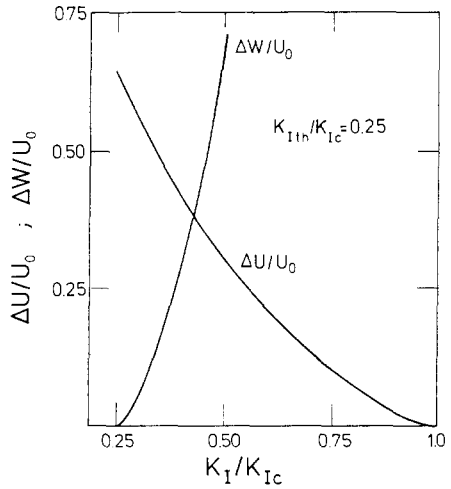

Fig. 4. Potential barriers $\Delta U/U_0$, $\Delta W/U_0$.

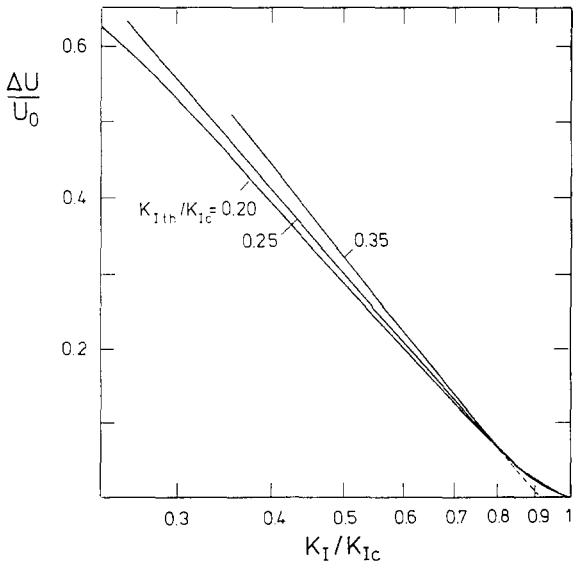

Fig. 5. Potential barrier $\Delta U/U_0$.

Table 1. Parameters of fitted straight lines

$K_{I\text{th}}/K_{Ic}$	A_0	A_1
0.2	−0.0386	−0.4722
0.25	−0.0432	−0.4948
0.30	−0.0460	−0.5152
0.35	−0.0473	−0.5337

The straight lines fitted to the curves indicate the coefficients of Table 1.

For interpolation these results are approximately expressed by

$$A_0 \simeq -0.00396 - 0.2393\frac{K_{I\text{th}}}{K_{Ic}} + 0.33\left(\frac{K_{I\text{th}}}{K_{Ic}}\right)^2 \tag{23}$$

and

$$A_1 \simeq -0.36155 - 0.6353\frac{K_{I\text{th}}}{K_{Ic}} + 0.40\left(\frac{K_{I\text{th}}}{K_{Ic}}\right)^2. \tag{24}$$

3. Crack propagation rates

Due to the thermal transients occurring at a frequency of N_0 shocks per unit of time, this bond will break after a time span on the order of

$$t \simeq \frac{1}{N_0}\exp(\Delta U/kT) \tag{25}$$

after a shock with a sufficiently high energy. However, this breaking is not necessarily a definite one. Only after a time t_0 – on the order of the time span required by the elastic waves to advance by one bond distance – the next bond undergoes mechanical stress and the crack tip will advance by one bond length.

As a result of the intensified retreat of the crack borders at the point of the previously broken bond, the two bonding partners are definitely separated (ΔW rises steeply). Thus, only during the time t_0 temporarily broken bonds can be closed again by new thermal transients.

The probability $\Delta N_\uparrow$ that during the interval Δt the bond at the crack tip opens, can be expressed by

$$\Delta N_\uparrow = N_0 \exp(-\Delta U/kT)\,\Delta t. \tag{26a}$$

On the other hand, the probability that the previously opened bond is restored during the characteristic time span t_0 becomes

$$\Delta N_\downarrow = N_0 \exp(-\Delta W/kT)\,t_0. \tag{26b}$$

Consequently, the probability that during Δt the bond is opened permanently becomes

$$\Delta N = N_0 \exp(-\Delta U/kT)\left[1 - N_0 t_0 \exp\left(-\frac{\Delta W}{kT}\right)\right]\Delta t,$$

$$\simeq N_0 \exp\left(-\frac{\Delta U}{kT}\right)\left[1 - \exp\left(-\frac{\Delta W}{kT}\right)\right]\Delta t. \tag{27}$$

As $N_0 t_0$ takes the order of magnitude $N_0 t_0 \simeq 1$ and, moreover, for the limit case $\Delta W \to 0$ the 'threshold condition' $\mathrm{d}N/\mathrm{d}t = 0$ should be satisfied, in (27) t_0 was chosen to be $t_0 = 1/N_0$.

In case of relative small load the crack growth rate is proportional to the rate $\Delta N/\Delta t$ [7]

$$v = \frac{\mathrm{d}a}{\mathrm{d}t} \propto \frac{\Delta N}{\Delta t}. \tag{28}$$

Directly at K_{Ic} the energy ΔU vanishes, all bonds are immediately broken and the crack growth rate must increase dramatically. This behaviour is modelled by (29) where at K_{Ic} the denominator becomes zero.

$$v = v_0 \frac{\exp\left(-\frac{\Delta U}{kT}\right)\left[1 - \exp\left(-\frac{\Delta W}{kT}\right)\right]}{1 - \exp\left(-\frac{\Delta U}{kT}\right)\left[1 - \exp\left(-\frac{\Delta W}{kT}\right)\right]}. \tag{29}$$

From (29) it can be seen that as the stress on a crack decreases, the expression in brackets becomes zero, and the crack-growth rate becomes zero too. The stress intensity factor value associated with this condition is K_{th}. In Fig. 6 the result of (29) is plotted as $\ln v/v_0$ versus $K_{\mathrm{I}}/K_{\mathrm{Ith}}$ for various values of $K_{\mathrm{Ith}}/K_{\mathrm{Ic}}$.

Since the terms containing ΔW vanish very rapidly when K_{I} exceeds K_{Ith} it holds in a wide range between $K_{\mathrm{Ith}}$and K_{Ic}:

$$\ln\frac{v}{v_0} = -\frac{U_0}{kT}\left[A_0 + A_1 \ln\left(\frac{K_{\mathrm{I}}}{K_{\mathrm{Ic}}}\right)\right]. \tag{30}$$

This can be written as

$$v = AK_{\mathrm{I}}^n, \tag{31}$$

where

$$A = \frac{v_0}{K_{\mathrm{Ic}}^n} \exp\left[-\frac{U_0 A_0}{kT}\right] \tag{32}$$

and

$$n = -\frac{A_1 U_0}{kT}. \tag{33}$$

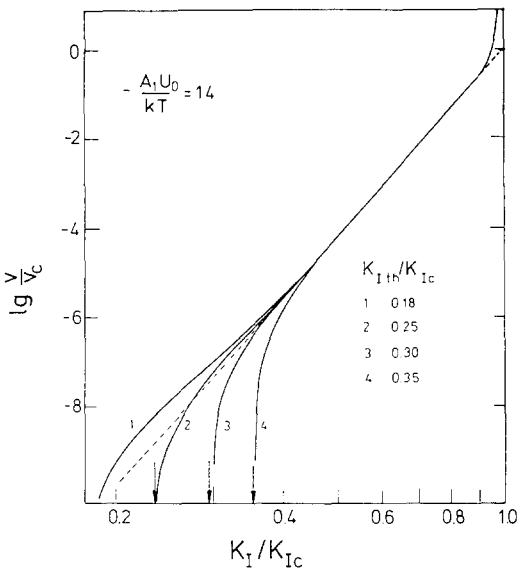

Fig. 6. Crack-growth rates computed with (29).

4. Comparison with experimental results

Crack growth results on soda-lime glass obtained by Wiederhorn and Bolz [11] have been plotted in Fig. 7. These data were determined in water of 25°C. The curve resulting from (29) for $K_{Ith}/K_{Ic} = 0.29$ and $n = -A_1U_0/kT = 16.5$ is additionally shown in Fig. 7. There is a good agreement with theory.

Figure 8 represents the results of three measurements made by Evans [12] on the same system, together with the curve computed for $K_{Ith}/K_{Ic} = 0.23$ and $n = -A_1U_0/kT = 14$. A very

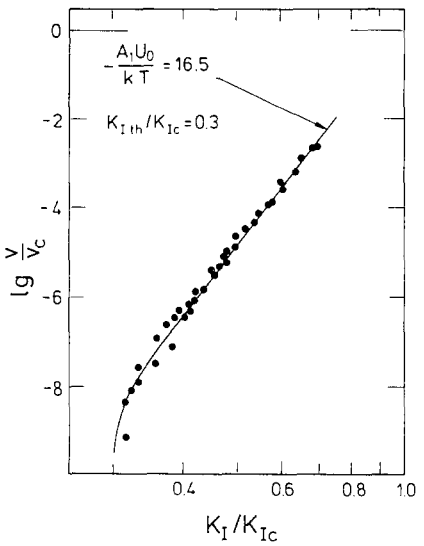

Fig. 7. Comparison of the crack growth rate v calculated according to (29) with experimental values for glass – measured by Wiederhorn and Bolz [11].

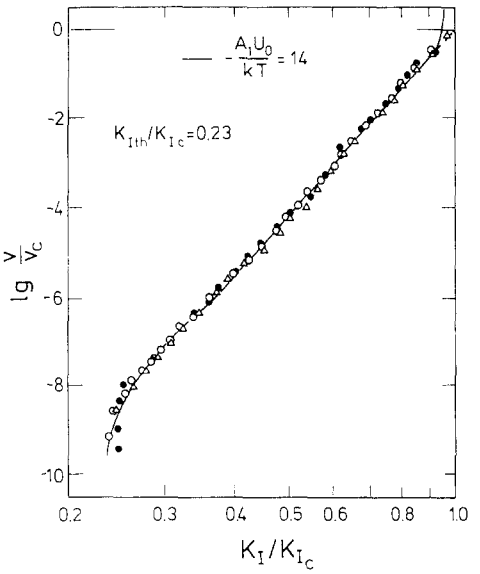

Fig. 8. Comparison of the crack growth rate v calculated according to (29) with experimental values for glass – measured by Evans [12] (different symbols indicate different specimens).

good agreement between measurements and theory is evident. It should be noted here that the normalisation $v(K)/v(K_{Ic})$ of the crack velocities on the slightly differing $v(K_{Ic})$-values characteristic of the three measuring series causes the measurement points to occur more closely to each other than in the original work.

Furthermore, it is interesting to note that both the theory and the experiment exhibit a slight hump-shaped deviation from linearity.

5. Influence of an environment

If medium is present at the crack tip this can change the potential barrier. Especially water with its high dielectric coefficient and high dipol moment will reduce the energy which is necessary for bond breaking. If the coefficient of reduction is denoted by κ and the potential barrier in the presence of the environment by ΔU_{env}, it holds

$$\Delta U_{env} = \kappa \Delta U, \quad \kappa < 1. \tag{34}$$

This value has to replace ΔU in (30), leading to an increased value of the factor A and a lower value of the crack growth exponent n:

$$A = \frac{v_0}{K_{Ic}^n} \exp\left[-\kappa \frac{U_0 A_0}{kT}\right] \tag{35}$$

and

$$n_{env} = -\kappa \frac{A_1 U_0}{kT}. \tag{36}$$

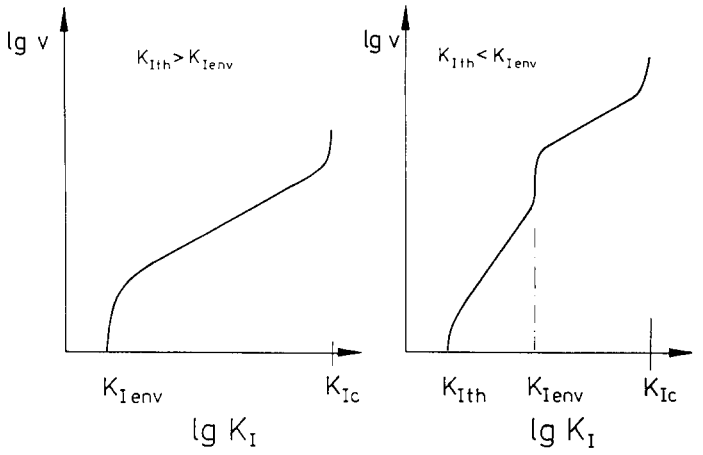

Fig. 9. Crack growth curves with different thresholds.

For this influence of the environment to be exerted a minimum value of K_I is necessary. If the molecule of the environment is replaced by a sphere with an effective radius R, the crack-opening displacement at distance R ahead of the crack tip must be at least $\delta(x = a - R) \geqslant R$.

From (7) it follows that the minimum stress intensity factor for an influence of the environment K_{Ienv} getting effective is

$$K_{Ienv} \geqslant E\sqrt{\frac{\pi}{8}R}. \tag{37}$$

This stress intensity factor value constitutes a second threshold value for subcritical crack growth which is independent of the value K_{Ith}. In Fig. 9 the influence of K_{Ienv} and K_{Ith} on the da/dt vs. K_I curve is illustrated. If $K_{Ienv} < K_{Ith}$ only K_{Ienv} governs the start of subcritical crack growth (Fig. 9a). In case of $K_{Ienv} > K_{Ith}$ an additional step in the crack growth curve has to be expected (Fig. 9b).

Appendix

The case $B = 0$ is illustrated by the left hand F-δ-diagram of Fig. 1. Substituting $z = \exp(-s\delta)$ in (13) yields the quadratic equation

$$z^2 - z + \frac{F}{4F_0} = 0$$

from which the two solutions

$$z_{1/2} = \tfrac{1}{2}(1 \pm \sqrt{1 - F/F_0})$$

or

$$s\delta^{(1),(2)} = \ln 2 - \ln(1 \pm \sqrt{1 - F/F_0})$$

result. The barrier ΔU (shaded area in Fig. 1) is given by

$$\Delta U = \int_{\delta^{(1)}}^{\delta^{(2)}} F(\delta)\,\mathrm{d}\delta - F(\delta^{(1)})\cdot(\delta^{(2)} - \delta^{(1)})$$

and consequently by

$$\frac{\Delta U}{U_0} = \sqrt{1-\beta} - \beta\ \mathrm{artanh}\sqrt{1-\beta} \quad \text{with} \quad \beta = F(\delta^{(1)})/F_0.$$

References

1. A.G. Evans, *Journal of Materials Science* 7 (1972) 1137–1146.
2. S.M. Wiederhorn, H. Johnson, A.M. Diness and A.H. Heuer, *Journal of American Ceramic Society* 57 (1974) 336–341.
3. S.M. Wiederhorn and L.H. Bolz, *Journal of the American Ceramic Society* 57 (1970) 543–548.
4. E.R. Fuller and R.M. Thomson, in *Fracture Mechanics of Ceramics* IV, Plenum Press (1978) 507–548.
5. B.R. Lawn, *Journal of Materials Science* 10 (1975) 469–480.
6. A.S. Krausz and J. Mshana, *International Journal of Fracture* 19 (1982) 277–293.
7. T. Fett and D. Munz, "Zur Deutung des unterkritischen Rißwachstums in keramischen Werkstoffen", DFVLR-Forschungsbericht FB 83-07, Cologne (1983).
8. H. Bueckner, in *Mechanics of Fracture I–Methods of Analysis and Solution of Crack Problems*, G.C.Sih (ed.), Noordhoff, Leyden (1979).
9. J.R. Rice, *International Journal of Solids and Structures* 8 (1972) 751–758.
10. H. Tada, *The Stress Analysis of Cracks Handbook*, Del Research Corporation (1986).
11. S.M. Wiederhorn and L.H. Bolz, *Journal of American Ceramic Society* 53 (1970) 543–548.
12. A.G. Evans, *Journal of Materials Science* 7 (1972) 1137–1146.